Supplementary file

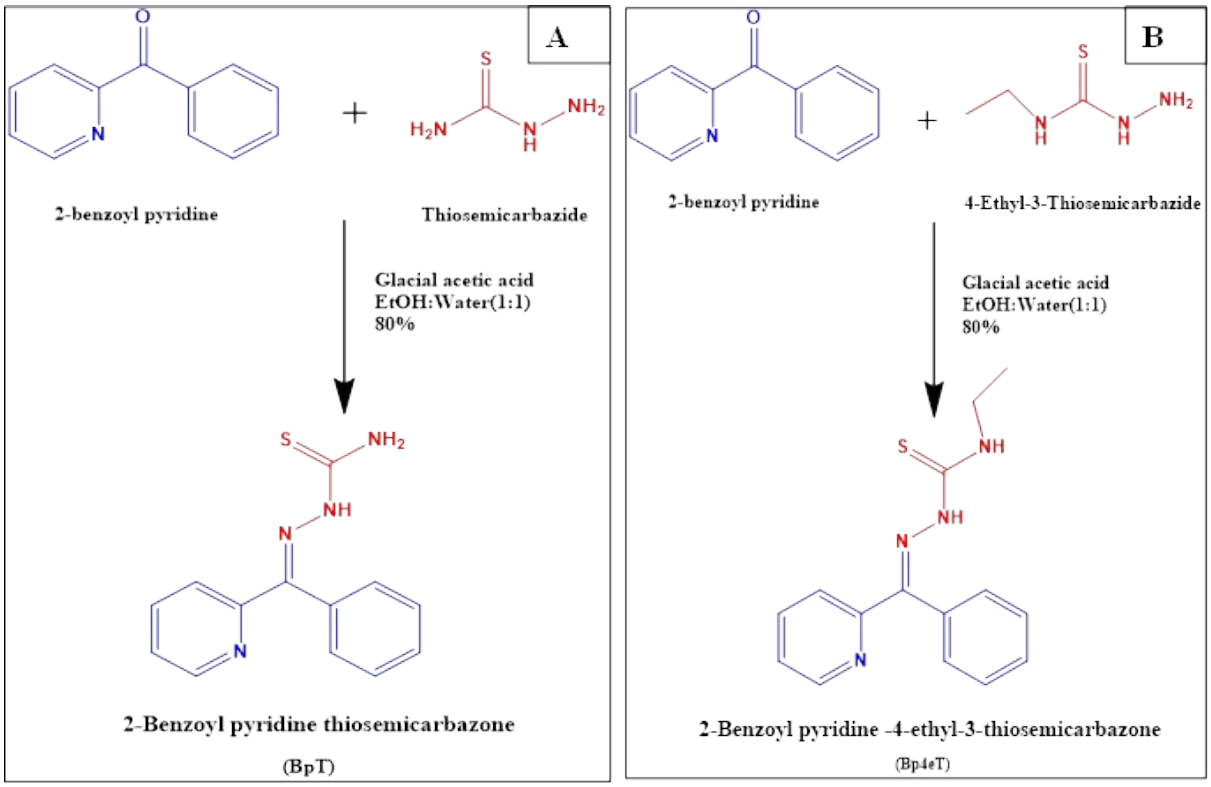

SchemeS1 : Synthesis of 2-Benzoyl pyridine thiosemicarbazone (BpT) and 2-Benzoyl pyridine-4-ethyl-3-thiosemicarbazone (Bp4eT)

1. Chemical characterization of BpT and Bp4eT

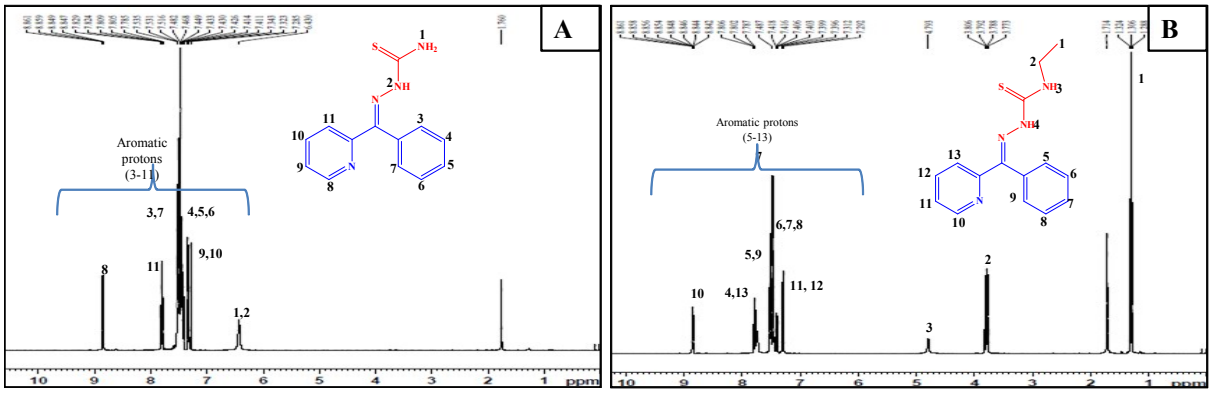

Figure S1: ^{1}H NMR spectra of BpT (A) and Bp4eT (B)

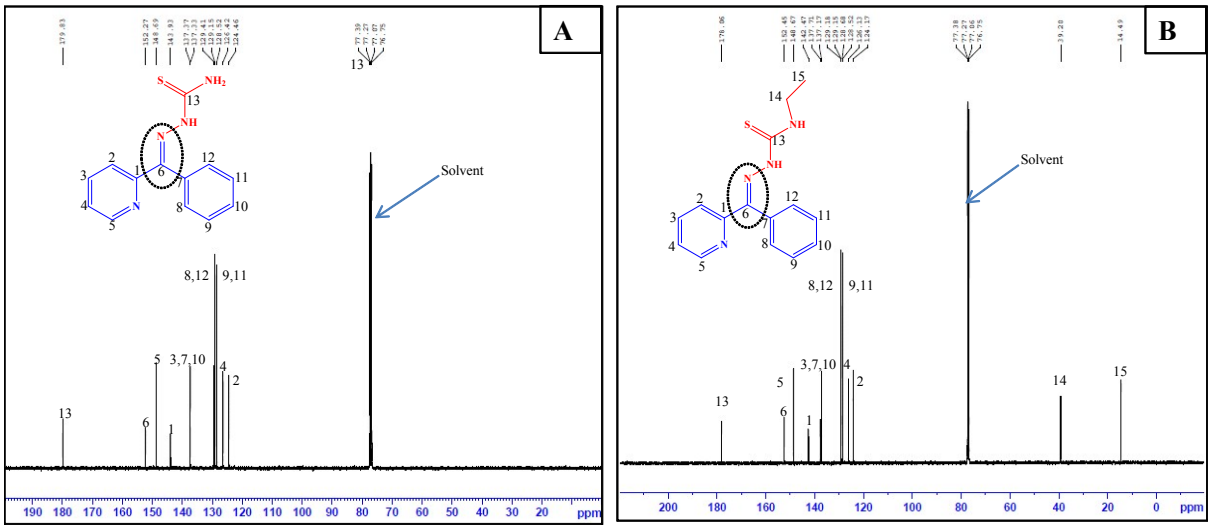

Figure S2: ^{13}C NMR spectra of BpT (A) and Bp4eT (B)

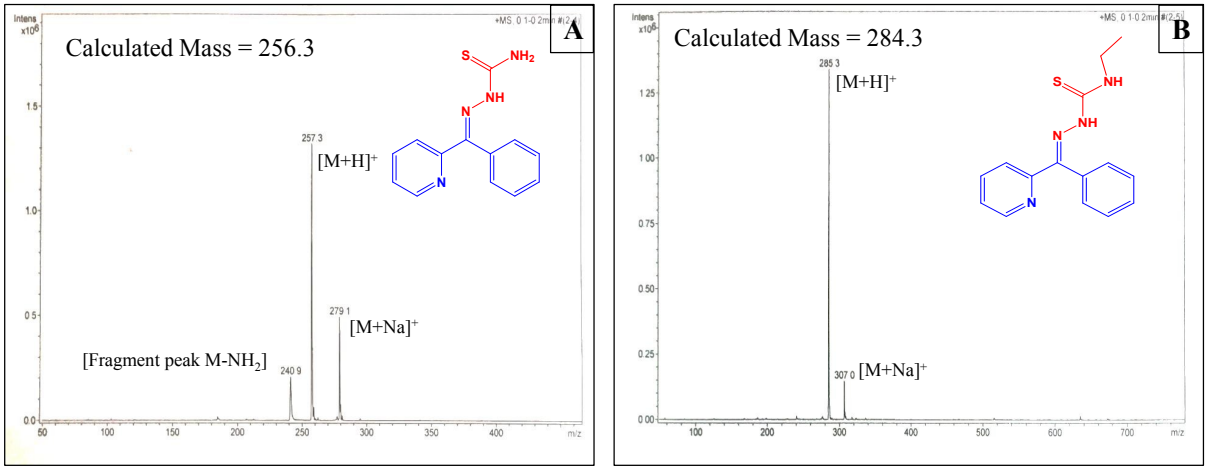

Figure S3: Mass spectra of BpT (A) and Bp4eT (B)

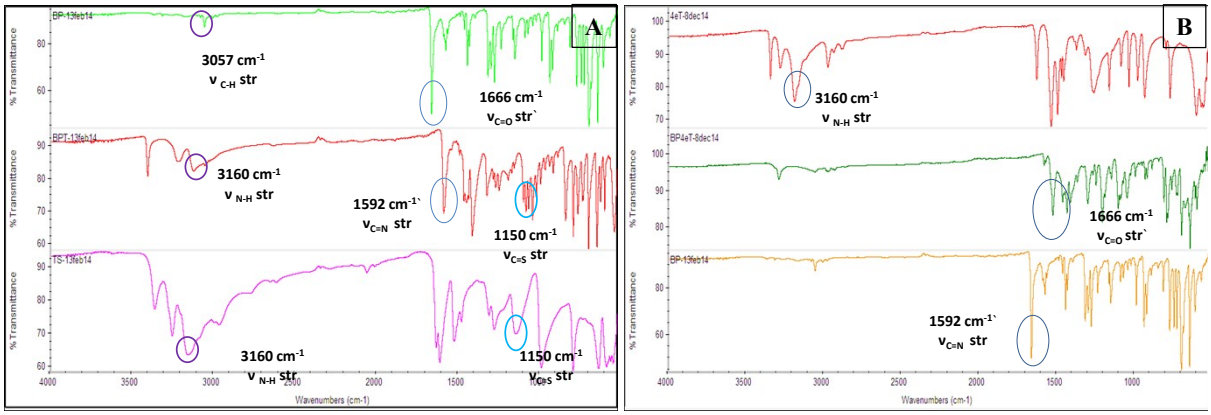

Figure S4: FTIR spectra of BpT (A) and Bp4eT (B)

2. Characterization of BpT and Bp4eT by UV/Vis spectroscopy

Electronic Spectra: UV-Vis spectroscopic analysis of the precursor i.e. 2-benzoyl pyridine (BP) at different concentrations of the precursor in ethanol, starting from 1mg/ml to 0.001mg/ml, gave a clear absorbance maxima at 269 nm which can be attributed to $\pi \rightarrow \pi^*$ transitions of benzene ring and conjugated pyridine ring through the intervening carbonyl group respectively.

The synthesis product BPT and BP4eT, were dissolved in organic solvent (chloroform). Their spectra exhibited a broad band around 330 nm owing to $n \rightarrow \pi^*$ and $\pi \rightarrow \pi^*$ transitions of imine and thioamide region of thiosemicarbazone moieties. No absorbance was observed around 269 nm, characteristic peaks of the precursors, indicating the total conversion of benzoylated pyridine to its Schiff's base product i.e. thiosemicarbazone.

References:-

[1] Fostiak L.M, Garcia I, Swearingen JK, Bermejo E Castineiras A, West DX (2003) Structural and spectral characterization of transition metal complexes of 2-pyridine formamide N(4)-dimethylthiosemicarbazone. Polyhdron 22:83 92. Doi: 10.1016/S02775387(02)01330-X

[2] Beraldo H, Boyd L.P, West DX (1998) Copper (II) and nickel (II) complexes of glyoxaldehyde bis-[N(3)-substituted thiosemicarbazones. Transit Met Chem 23:67 71.doi:10.1023/A:1006958018049

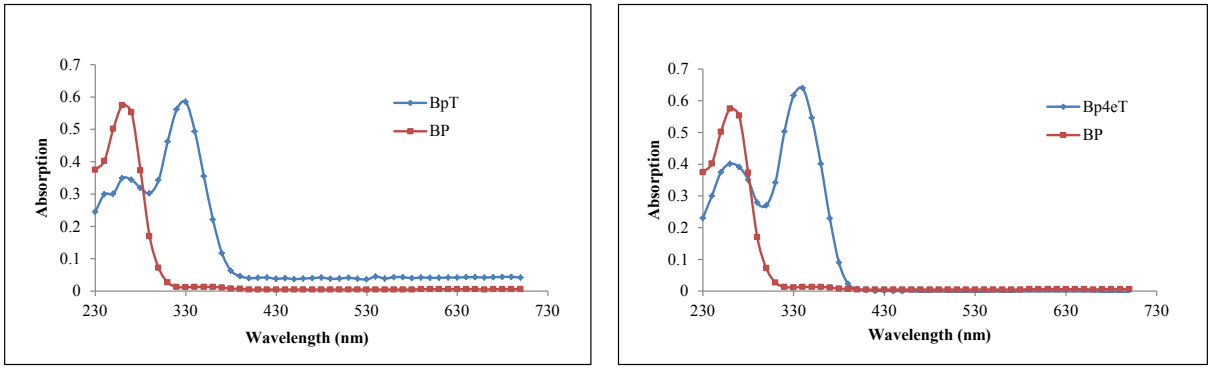

Figure S5 : UV profile of BpT and Bp4eT in comparison with BP

3. Calibration curves of BPT and BP4eT in acetate buffer(pH 5.5) and PBS(pH 7.4, 0.1M)

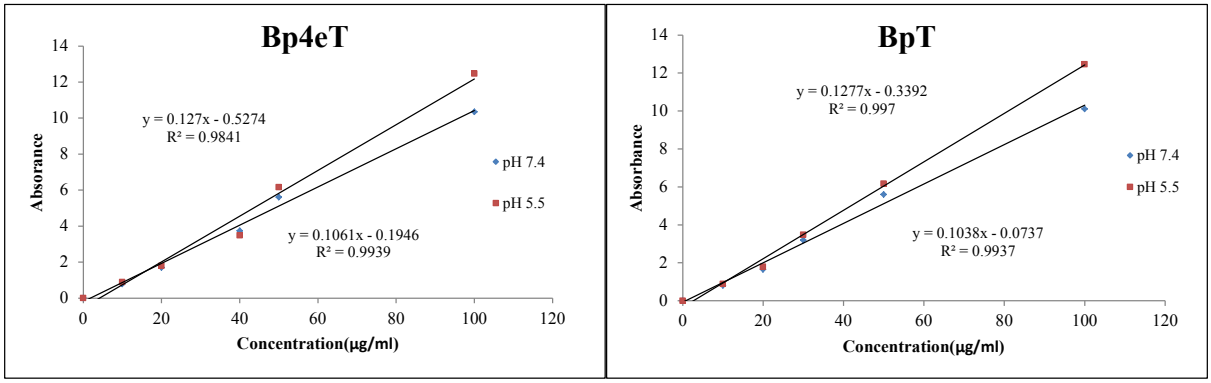

Figure S6 : Calibration curves of BpT and Bp4eT

4. Model fitting for drug release kinetics

The release data of BPT-PB-SLNs and BP4eT-PB-SLNs did not show a good fit with first order and Higuchi models.

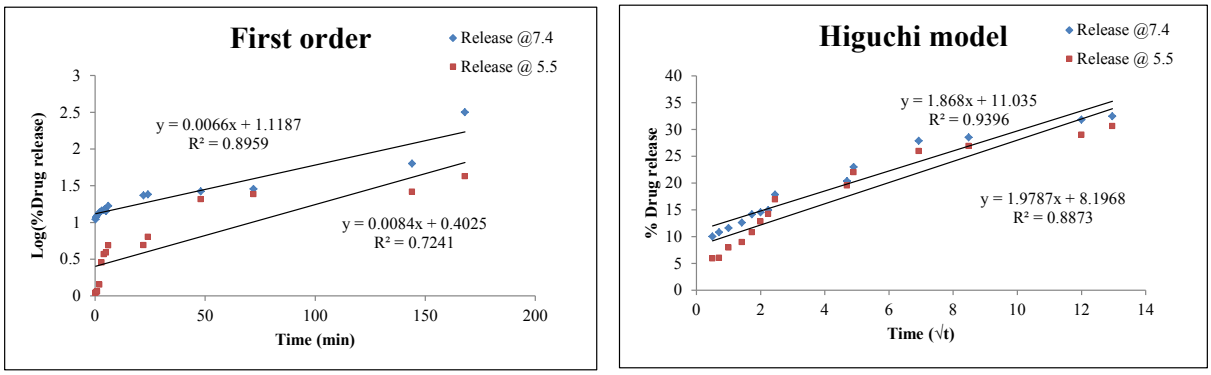

Figure S7a : In-vitro drug release profile ananlyzed by kinetics models (First order and Higuchi model) of BPT-BP-SLNs

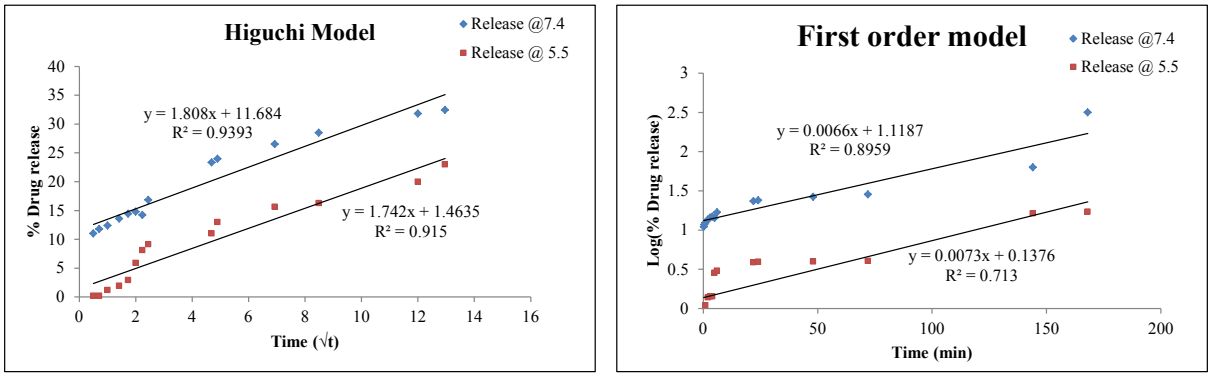

Figure S7b : In-vitro drug release profile ananlyzed by kinetics models (First order and Higuchi model) of BP4eT-BP-SLNs

5. Quality control of radiolabelled compounds:

It was essential to estimate the purity of the ^{99m}Tc-labelled BpT-PB-SLNs and Bp4eT-PB-SLNs compounds, which were easily performed chromatographically using ITLC-SG strips as the stationary phase and 100% acetone as the mobile phase. A spot of the reaction mixture was made on the ITLC-SG strip at the bottom and was allowed to run in 100% acetone. It was seen that the free pertechnetate ($^{99m}TcO_4^-$) moved with the solvent front while the radiolabelled compound stays at the point of application, along with the reduced or hydrolyzed colloids. Later, when PAW was used as the solvent front instead of acetone, the radiolabelled complex also moved along with the solvent and only the reduced or hydrolyzed colloids remained at the bottom (at the point of application). The difference in the counts obtained by using acetone and PAW depicts the percentage of ^{99m}Tc-labelled BpT-PB-SLNs and Bp4eT-PB-SLNs compounds formed. Both the compounds demonstrated more than 99% of radiolabelling efficiency at an optimum pH of 7.

Optimization of radiolabeling efficiency

Prior to use of the labeled complexes, various factors influencing the labeling efficiency of the complexes were studied. *pH of the formulation* is an important factor that affects the radiolabelling efficiency significantly. pH of the mixture was varied in the range of 3.5 to 7.5, keeping all the other parameters constant and the corresponding efficiency was measured. From Figure S4, it was observed that the radiolabelling efficiency was considerably high for both the complexes at a pH of **7.**

Concentration of $SnCl_2$ solution, used to reduce technetium, also affects the stability as well as the radiolabeling efficiency of the complexes. On varying the $SnCl_2$ concentrations in the range of 50 to 400µg, keeping all the other factors constant, it was found that the labeling efficiency was highest when the $SnCl_2$ concentration was **300µL** for both the complexes.

Similarly, on varying the *temperature* at which the labeling procedure (25-40°) was carried out and calculating the corresponding radiolabeling efficiency for determining the optimum temperature, it was found that the highest efficiency was obtained at **35 ºC**.

The *incubation time* of the radiolabeled mixture was also optimized by incubating the reaction mixture for different time durations varying from 10mins to 40mins and on calculating the corresponding labeling efficiencies, it was found that the optimum incubation time of **30mins** gave the highest labeling efficiency.

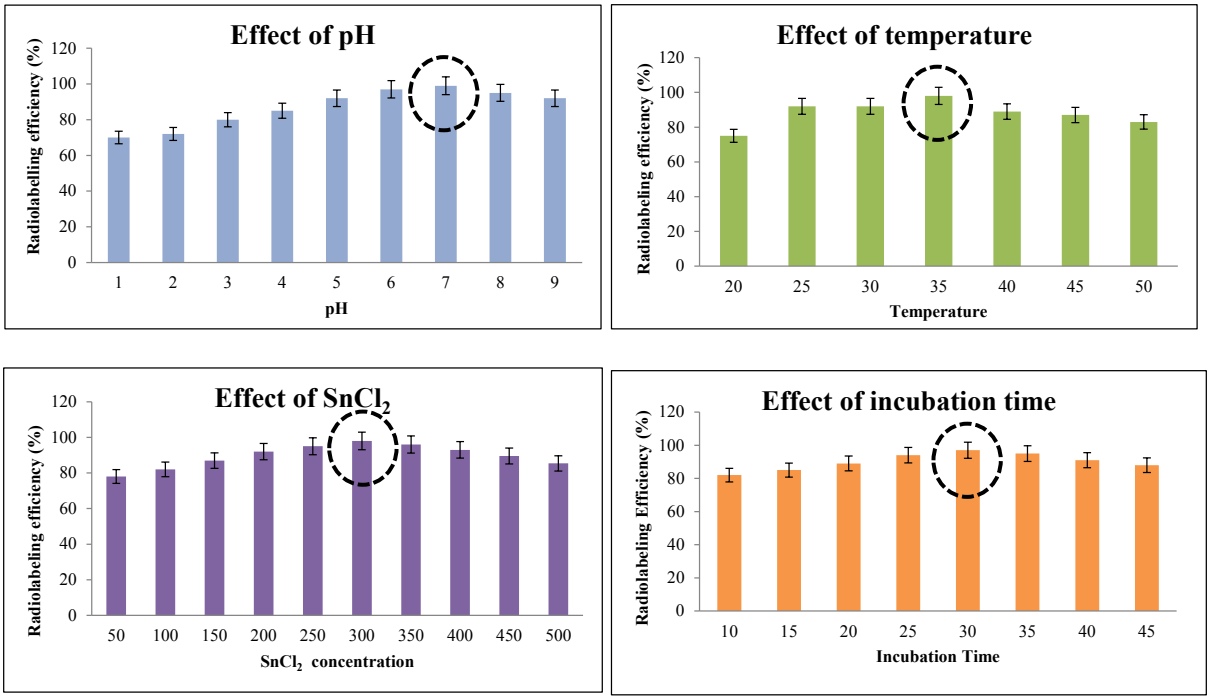

Figure S8 : Optimization of different radiolabelling parameters (pH, temperature, concentration of $SnCl_2$ and incubation time) of BpT-PB-SLNs and Bp4eT-PB-SLNs

6. In vitro serum stability

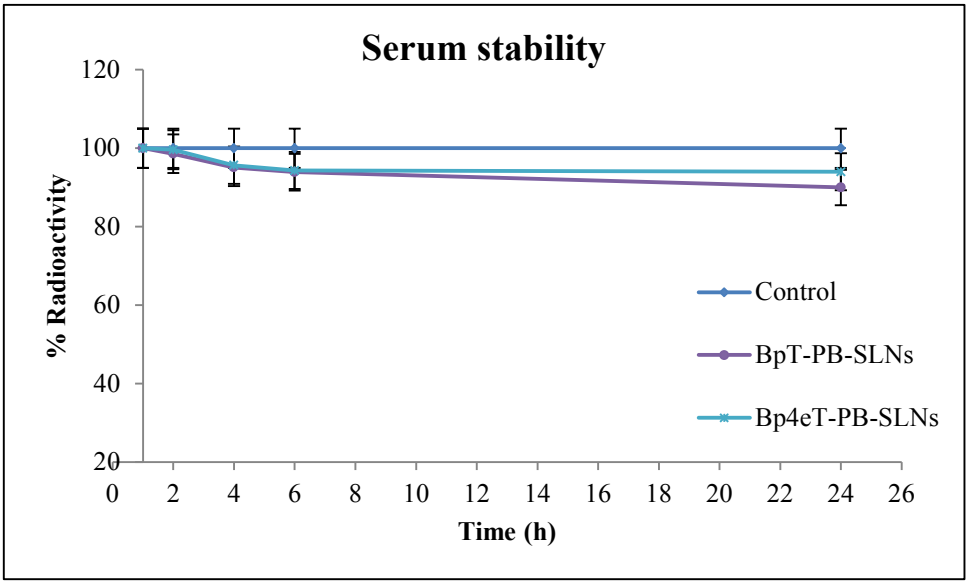

Figure S9: In-vitro serum stability of ^{99m}Tc labeled BpT-PB-SLNs and Bp4eT-PB-SLNs

7. Biodistribution studies of BpT and Bp4eT iron chelators

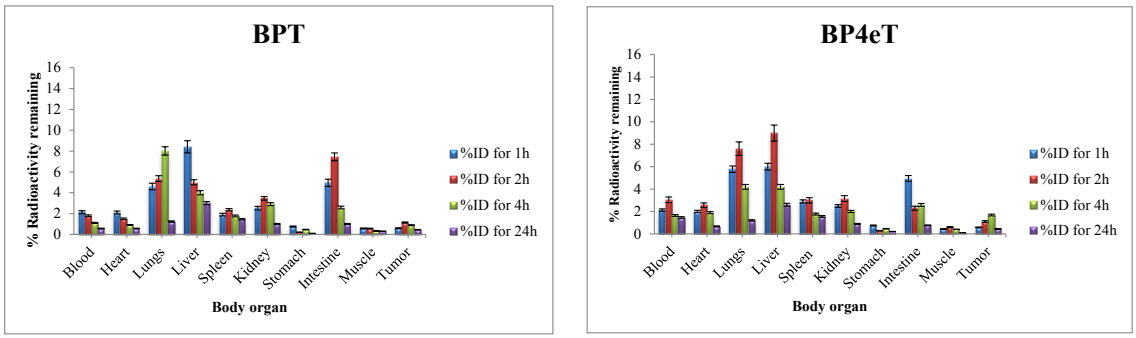

Figure S10: Biodistribution profile of 99mTc labeled (a) BPT and (b) Bp4eT iron chelators, respectively.